Accepted Manuscript

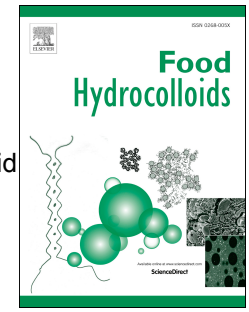

Effect of pH and salts on microstructure and viscoelastic properties of lemon peel acid insoluble fiber suspensions upon high pressure homogenization

Katleen L.D.D. Willemsen, Agnese Panozzo, Katlijn Moelants, Ruth Cardinaels, Joel Wallecan, Paula Moldenaers, Marc Hendrickx

PII: S0268-005X(18)30009-2

DOI: 10.1016/j.foodhyd.2018.04.005

Reference: FOOHYD 4372

To appear in: *Food Hydrocolloids*

Received Date: 3 January 2018

Revised Date: 29 March 2018

Accepted Date: 1 April 2018

Please cite this article as: Willemsen, K.L.D.D., Panozzo, A., Moelants, K., Cardinaels, R., Wallecan, J., Moldenaers, P., Hendrickx, M., Effect of pH and salts on microstructure and viscoelastic properties of lemon peel acid insoluble fiber suspensions upon high pressure homogenization, *Food Hydrocolloids* (2018), doi: 10.1016/j.foodhyd.2018.04.005.

This is a PDF file of an unedited manuscript that has been accepted for publication. As a service to our customers we are providing this early version of the manuscript. The manuscript will undergo copyediting, typesetting, and review of the resulting proof before it is published in its final form. Please note that during the production process errors may be discovered which could affect the content, and all legal disclaimers that apply to the journal pertain.


Extensive
pectin extraction
Optimal
viscoelastic properties

pH 4.5-pH 7

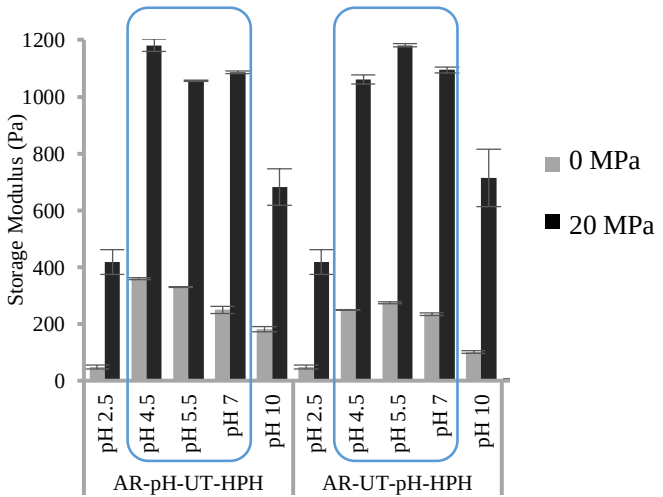
Storage Modulus (Pa)
1200
1000
800
600
400
200
0
pH 2.5
pH 4.5
pH 5.5
pH 7
pH 10
pH 2.5
pH 4.5
pH 5.5
pH 7
pH 10
AR-pH-UT-HPH
AR-UT-pH-HPH
0 MPa
20 MPa

ACCEPTED MANUSCRIPT

Effect of pH and salts on microstructure and viscoelastic properties of lemon peel acid insoluble fiber suspensions upon high pressure homogenization

Authors: Katleen L.D.D. Willemsen[a], Agnese Panozzo[a], Katlijn Moelants[b], Ruth Cardinaels[c], Joel Wallecan[b], Paula Moldenaers[c] and Marc Hendrickx[a]

Authors' affiliation:

[a] Laboratory of Food Technology, Leuven Food Science and Nutrition Research Centre (LFoRCe), Department of Microbial and Molecular Systems (M^2S), KU Leuven, Kasteelpark Arenberg 22, Box 2457, 3001 Leuven, Belgium

[b] Cargill R&D Centre Europe, Havenstraat 84, 1800 Vilvoorde, Belgium

[c] Soft Matter, Rheology and Technology (SMaRT), Department of Chemical Engineering (CIT), KU Leuven, Celestijnenlaan 200F, box 2424, 3001 Leuven, Belgium

*Corresponding author: marceg.hendrickx@kuleuven.be

ACCEPTED MANUSCRIPT

ACCEPTED MANUSCRIPT

Abstract

In the present paper the effect of pH and salts on microstructural and viscoelastic properties of lemon peel acid insoluble fiber residue (AR) suspensions upon mild and intense shearing was investigated. To this aim, AR suspensions were adjusted to a pH of 2.5 (as is), 4.5, 5.5, 7 or 10 prior to or after high pressure homogenization (HPH) at 20 MPa (high shearing), with or without blending (low shearing). Furthermore, the effect of salts was investigated by addition of NaCl or $CaCl_2$ to the AR suspensions upon blending and HPH. Microstructural characterization of the AR suspensions, was performed through microscopic visualization and determination of the particle size distribution by laser diffraction, whereas viscoelastic properties were determined by rheological analysis.

Regardless of the pH conditions, blending prior to HPH was essential to obtain optimally functionalized AR suspensions. Furthermore, the effect of the sequence of blending and pH adjustment was negligible, whereas pH adjustment played a crucial role prior to HPH. In particular, increasing the pH above its intrinsic condition (pH 2.5) assisted the functionalization of AR suspensions by HPH, improving its viscoelastic properties. Contrarily, high salt concentrations negatively influenced the functionalization of AR suspensions. This effect of pH and salts was attributed to changes in electrostatic forces between AR fibers due to the presence of negative charged residual pectin polymers, favoring fiber separation (upon HPH) and increasing its hydration potential. On the other hand, high salt concentrations will shield AR fiber charges, thereby reducing the viscoelastic properties of the fiber suspensions.

Keywords: High pressure homogenization, pH, microstructure, viscoelastic properties, cell wall fibers

ACCEPTED MANUSCRIPT

1. Introduction

In the last decades, the increase in consumer interest in health and environmental issues has boosted the demand for overall natural and sustainable food products and ingredients with technological and/or health-related properties. In this context, the integrated use of fruit and vegetable by-products provides an interesting solution for reducing food waste, enriching food products with dietary fibers, and generating natural texturizers, thus meeting the environmental, nutritional, and technological consumer requirements. Despite the abundance of fruit and vegetable by-products, their exploitation as natural food ingredients is still limited. The under-exploitation of fruit and vegetable based by products is partly caused by the complex three-dimensional network of cell wall fibers. Such network is made of cellulose fibrils embedded in a matrix of pectin and hemicellulose (Cosgrove, 2005). The cellulose fibrils are immobilized by intra- and intermolecular hydrogen bonding and hydrophobic interactions, while pectin and hemicellulose are characterized by a higher degree of mobility (Cosgrove, 2014). Within this polysaccharide network a small amount of protein is also included (Lamport, Kieliszewski, Chen, & Cannon, 2011; Sampedro & Cosgrove, 2005). To unlock the full structuring potential of these fibers, the compact cell wall fiber network must be unraveled, allowing for better hydration and swelling of the fibers.

Functionalization of plant cell wall material can be achieved by mechanical treatments (Foster, 2011). In this context, high pressure homogenization has been shown to affect the functionality of plant-based material by both reducing the particle dimension as well as enabling fiber network formation (Augusto, Ibarz, & Cristianini, 2013; Lopez-Sanchez et al., 2011; Tan & Kerr, 2015; Van Buggenhout et al., 2015; Winuprasith & Suphantharika, 2013). During high pressure homogenization a fluid is forced through a narrow gap in the homogenizer valve, where it undergoes a rapid acceleration (Dumay et al., 2013; Floury, Legrand, & Desrumaux, 2004). Consequently the fluid is subjected to cavitation, shear and turbulence phenomena that are simultaneously induced, and lead to a temperature increase depending on the applied pressure (Paquin, 1999). Recent results of Willemsen et al. (2017) proved high pressure homogenization to be effective in increasing the viscoelastic properties (i.e. storage modulus) of lemon peel fiber suspensions, after extensive pectin removal. Moreover, extensive pectin removal was found to be crucial in the functionalization of lemon peel fiber suspensions, having very low viscoelastic properties as such. Similarly, Sankaran et al. (2015) reported that the enzymatic degradation of pectin favored the loosening of carrot cell wall fibers upon high pressure homogenization. In addition to the remaining pectin content, the viscoelastic properties of fiber suspensions depend not only on their composition, but also on their physicochemical characteristics (Kunzek, Müller, Vetter, & Godeck, 2002). Therefore, any intrinsic system properties affecting these characteristics, such as pH and presence of salts, is likely to influence the mechanical processing effects (Sankaran, Nijsse, Bialek, Shpigelman, et al., 2015; Shpigelman, Kyomugasho, Christiaens, Van Loey, & Hendrickx, 2014).

In light of these considerations, the aim of the present work was to investigate the effect of pressure level, pH, and salts on the microstructural and viscoelastic properties of pectin depleted lemon peel fiber suspensions upon mild and intense shear mechanical treatments. To this aim, lemon peel fibers were subjected to pectin extraction under acidic conditions. The resulting insoluble fibers were suspended in standardized tap water (2%, w/w), adjusted to different pH and conductivity values by the addition of salts and subjected to blending (low mechanical shear) and high pressure homogenization (high mechanical shear).

ACCEPTED MANUSCRIPT

2. Materials and Methods

2.1 Raw materials and reagents

Lemon peel was received in dried and milled state from a local supplier. Extraction of the alcohol insoluble residue (AIR) from lemon peel was performed using ethanol (C_2H_5OH, technical, Chem-lab, Zedelgem, Belgium) and acetone (C_3H_6O, technical, VWR, Pennsylvania, USA). Acid pectin extraction on the AIR was performed using 7N nitric acid (HNO_3, 65%, Merck, New Jersey, USA). Furthermore, standardized tap water containing 0.2% sodium chloride (NaCl, analytical grade, Fisher scientific, New Hampshire, USA) and 0.015% dehydrated calcium chloride ($CaCl_2{\cdot}H_2O$, 99.5%, Chem-lab, Zedelgem, Belgium) in ultrapure water (organic free, 18 MΩ cm resistance), supplied by a Simplicity™ water purification system (Millipore, Billerica, USA), was used to make AR suspensions. Either sodium carbonate ($NaCO_3$, 99.8%, VWR, Pennsylvania, USA) or hydrochloric acid (HCl, Fisher scientific, New Hampshire, USA) was used for pH adjustments whereas sodium chloride (NaCl, analytical grade, Fisher scientific, New Hampshire, USA) or calcium chloride ($CaCl_2{\cdot}H_2O$, 99.5%, Chem-lab, Zedelgem, Belgium) was used to increase the salt content. Acridine orange (Sigma-Aldrich, Missouri, USA) was used to stain cell wall polymers for epifluorescence microscopy.

2.2 Experimental design

The aim of the present work was to investigate the effect of processing variables (pressure level) as well as intrinsic system properties, namely pH and salts, on the microstructural and functional properties of lemon peel acid insoluble fibers subjected to different sequences of processing operations. An acid pectin extraction was performed on dried lemon peel in order to remove most of the pectin therein. The lemon peel acid insoluble residue (AR), as obtained by acid extraction, was characterized by pH 2.3 and 6.5% dry matter content. Firstly, the effect of the homogenization pressure was investigated by suspending AR in a 2% (w/w) ratio with standardized tap water, adjusting the pH to pH 5.5 by the addition of sodium carbonate, blending and high pressure homogenization, ranging from 10 to 70 MPa. Subsequently, the effect of intrinsic system properties and sequence of processing operations was investigated. An overview of the experimental design is depicted in figure 1. In particular, the AR was suspended to 2% (w/w) with standardized tap water and adjusted to pH 2.5, 4.5, 5.5, 7.0, and 10.0 using sodium carbonate or hydrochloric acid. The AR suspension was either blended (sequence 1 and 2) or not (sequence 3). In the former case, the blending was performed either after (sequence 1) or before (sequence 2) the pH adjustment. Additional samples were prepared by adjusting the AR suspension to pH 4.5, blending, and readjusting the pH to 2.5 with HCl (sequence 4). Finally, the AR suspension was adjusted to pH 4.5 and conductivity of 8 mS/cm by addition of either NaCl or $CaCl_2$, and blended (sequence 5). Subsequently the obtained AR suspensions were homogenized at 20 MPa. Non-homogenized samples were considered as controls. The non-homogenized and homogenized lemon peel acid insoluble residue suspensions prepared following the different sequences of processing operations were characterized for their electrical conductivity as well as microstructural and functional properties.

120

121 **2.3 Lemon peel alcohol insoluble residue**

122 The cell wall material was isolated from lemon peel as the alcohol insoluble residue (AIR) using the
123 method described by McFeeters and Armstrong (1984). Approximately 30 g of lemon peel was wetted
124 with 30 g demineralized water. The wetted lemon peel was suspended in 192 ml 95% ethanol using a
125 mixer (3 times for 6 s) (Buchi mixer B-400, Flawil, Switzerland). The suspension was filtered over a
126 paper filter (Machery-Nagel MN 615 Ø 90 mm). Thereafter, the residue was resuspended in 96 ml
127 95% ethanol while mixing, and filtered again. Subsequently the residue was suspended in 96 ml
128 acetone using a magnetic stirrer and filtered to obtain the AIR (residue). The AIR was dried overnight
129 at 40 °C. The dried AIR was grounded with a mortar and pestle and stored in a desiccator until further
130 use.

131 **2.4 Lemon peel acid insoluble residue**

132 An acid extraction was performed to remove pectin from the AIR according to the protocol described
133 by Willemsen et al. (2017). In particular, 60 g of AIR was suspended in 4000 ml of distilled water and
134 incubated for 30 min at 80 °C under stirring. Subsequently, the pH of the suspension was adjusted to
135 1.6 with 7 N HNO_3, and the incubation was continued for another 60 min. Thereafter, the suspension
136 was cooled in an ice bath and centrifuged at room temperature for 10 min at 4000 g. The pectin rich
137 acid supernatant (AF) was separated and the pellet was washed with 1 L distilled water before
138 filtration over a paper filter (Machery-Nagel MN 615 Ø 90 mm). The lemon peel acid insoluble
139 residue (AR) was suspended in standardized tap water in a concentration of 2% (w/w). Thereafter, the
140 pH of the AR suspensions was adjusted to pH 2.5, 4.5, 5.5, 7.0 or 10 using a few drops of 2 M Na_2CO_3
141 or 1 M HCl under magnetic stirring. Magnetic stirring was performed overnight whereafter the final
142 pH was checked. Additional samples were prepared by adding NaCl or $CaCl_2$ to the AR suspension
143 until the conductivity of the suspension was equal to 8 mS/cm.

144 **2.5 Blending and high pressure homogenization of the lemon peel acid insoluble residue**

145 When including blending, AR suspensions were treated with an Ultra-Turrax (IKA, Staufen,
146 Germany) for 10 min at 8000 rpm prior to or after pH adjustment, to obtain a homogenous suspension.
147 Lemon peel acid insoluble residue suspensions adjusted to different pH and conductivity values, either
148 subjected or not subjected to blending, were homogenized using a high pressure homogenizer Pony
149 NS2006L (pH adjusted samples) or Panda 2k NS1001L (conductivity adjusted samples) (GEA Niro
150 Soavi, Parma, Italy) at 20 MPa. To identify the effect of homogenization pressure, AR suspensions
151 were adjusted to pH 5.5 prior to blending and high pressure homogenization (Panda 2k, GEA Niro
152 Soavi, Parma, Italy) at 10, 20, 30, 40, 50, 60 and 70 MPa. Non-homogenized samples (0 MPa) were
153 considered as control.

154 **2.6 Electrical conductivity measurement**

155 The electrical conductivity of the AR suspensions and of standardized tap water was measured at room
156 temperature with a portable EC/TDS conductometer (Orchids, France). The conductometer was

calibrated with the calibration solution provided with the device. Before the measurements, the homogenized AR suspensions were diluted 10 folds with MilliQ water and gently stirred to obtain a homogenous suspension. The conductivity values were then corrected for the dilution factor.

2.7 Particle size measurement

The particle size distribution was measured by laser diffraction (Beckman Coulter, LS 13 320, Miami, Florida). Samples were poured into a stirred tank filled with demineralized water and circulated two times into the measuring cell (pumping rate 30%). Each sample was analyzed in duplicate. Laser light of 750 nm was used as the main laser light source, whereas laser light having a wavelength of 450, 600, and 900 nm was used for polarization intensity differential scattering (PIDS). The detection range was 0.04-2000 µm. The volumetric particle size distributions and median particle diameter (D_{50}) of the samples were calculated from the intensity distributions of the scattered light according to the Fraunhofer optical model using the instrument's software (plant cell wall RI = 1.6, water RI = 1.33 and absorption coefficient for the dispersion = 1) (Verrijssen et al., 2014).

2.8 Microscopy analysis

The microstructure of the non-homogenized and homogenized samples was visualized by means of microscopy, using cell wall specific dyes and epifluorescent lighting, as well as normal light in differential interference contrast (DIC) mode. The samples for epifluorescence analysis were stained with acridine orange (dilution of 1:100 from 2% concentrated dye) and analyzed using an Olympus BX-41 microscope, equipped with an Olympus XC-50 digital camera and photo-analyzing software. Acridine orange was used as a cationic dye which associates with polyanionic compounds while emitting a green fluorescence. Several microscopic images were taken with objective 10 x to create a representative overview of the cell wall suspension.

2.9 Rheological analysis

Rheological measurements were performed with a stress controlled rheometer (MCR302, Anton Paar, Graz, Austria) at 25 °C. Samples were analyzed within 24 h after preparation and homogenization. A custom-built concentric cylinder with a conical bottom and cup were used. Both the cylinder and the cup were sand blasted resulting in an average surface roughness between 50 and 100 µm. The gap between the inner cylinder and the cup was 2 mm. For each measurement, 25 ml of sample was loaded into the cup. To avoid potential effects of sample manipulation and loading history on the measurements, the samples were pre-sheared at 10 s^{-1} for 30 s, and allowed to rest for 30 s before the measurements. Given the time required for the tests to be performed (20 to 30 min), solvent evaporation was considered to be negligible. Oscillatory measurements were performed to obtain information on the viscoelastic behavior of the samples. At first, a strain sweep from 0.01 to 1000% strain at an angular frequency of 6.28 rad/s was carried out to identify the linear viscoelastic region (LVR). Thereafter, frequency sweep tests were performed at a constant strain amplitude of 1% (within the LVR) from 628 to 0.628 rad/s to determine the dependence of the storage and loss moduli (G' and

G'') on the angular frequency. Frequency sweep measurements were performed in duplicate on a freshly loaded sample.

2.10 Statistical analysis

Results are expressed as mean ± standard deviation of at least two replicates. Analyses of variance (ANOVA) was performed with the significance level set on $P < 0.05$ (Statistica for Windows, ver. 5.1, Statsoft Inc. Tulsa, USA, 1997) whereas Tukey's procedure was used to test for differences between means.

3. Results and discussion

3.1 Effect of homogenization pressure

Recent work of Willemsen et al. (2017) showed that extensive pectin extraction, performed under alkaline (pH 10) or acid (pH 2.5) conditions, favors the viscoelastic properties (i.e. storage modulus) of lemon peel fiber suspensions differently. In both cases, the resulting system properties (pH and presence of salts) were substantially different, suggesting an influence of these system properties on the viscoelastic properties of lemon fiber residue suspensions. In addition, Willemsen et al. (2017) reported the importance of high pressure homogenization for the functionalization of lemon peel fiber suspensions. Therefore, the effect of homogenization pressure level on the viscoelastic properties of AR suspensions was evaluated in the first part of this research, prior to investigating the effects of intrinsic system properties and sequence of unit operations. To this aim, AR suspensions were adjusted to an intermediate pH of 5.5, followed by blending and high pressure homogenization at a pressure varying from 10 MPa to 70 MPa. A blended non-homogenized AR suspension was also included as control (0 MPa). Microstructural changes were visualized by light and epifluorescence microscopy, using acridine orange staining (figure 2). When considering the blended (0 MPa) AR suspension (figure 2), both light and epifluorescence micrographs show the presence of cell clusters. Upon high pressure homogenization at 10 MPa, these cell clusters are disrupted, resulting in a rather homogeneous distribution of the disrupted particles. Moreover, the AR cell wall material seemed to swell or interact to some extent, resulting in a more homogeneous overall green blurriness under fluorescence microscopy, using acridine orange staining. This AR fiber interaction, possibly caused by a rearrangement of the fibers or swelling, increased with the homogenization pressure up to 20 MPa, resulting in a more uniform distribution of the material. Based on microscopic analysis, further increase in homogenization pressure did not result in noticeable microstructural changes. Therefore, only a selection of microscopy images is shown in figure 2.

Furthermore, the effect of homogenization pressure on the microstructure of the AR suspensions was investigated by laser diffraction analysis. Since all samples were characterized by a monomodal particle size distribution with a similar span (data not shown), the median particle diameter (D_{50}) was considered for quantitative comparison (table 1). Compared with the high pressure homogenized AR suspensions, the non-homogenized AR suspension was characterized with a larger median particle diameter of 118 ± 1 µm. In good agreement with light and epifluorescence micrographs, the D_{50} of the

non-homogenized AR suspension indicate the presence of cell clusters. It is remarkable that, regardless of the homogenization pressure, the D_{50} of all homogenized AR suspensions was rather similar, ranging between values of 69 ± 0 and 78 ± 4 µm. Although microscopy showed an increased swelling or interaction of the AR material upon high pressure homogenization at 10 MPa and 20 MPa (figure 2), particle size analysis did not confirm this trend. In contrast to microscopy, laser diffraction analysis was carried out under highly diluted conditions and slight turbulence. Therefore, it is suggested that the interaction of homogenized AR material, observed during microscopic analysis, is caused by weak particle interactions and is therefore not apparent during laser diffraction analysis.

The functionality of the (non-)homogenized AR suspensions, expressed as their viscoelastic behavior, was determined by rheological analysis. The linear viscoelastic region, where the storage (G') and loss (G") moduli are independent of the strain, was determined for each AR suspension by performing strain sweep experiments (data not show). A constant strain of 1% (within the linear viscoelastic region of all suspensions) was selected to perform frequency sweep experiments for further viscoelastic characterization (figure A, supplementary data). For all samples, G' values were found to be higher than G" values, and G' was found to be rather independent of frequency. Therefore, functionality of the samples was compared based on the G' value at an angular frequency of 6.28 rad/s (figure 3). While the non-homogenized AR suspension is characterized with a G' value of only 194 ± 1 Pa, high pressure homogenization at 10 MPa and 20 MPa resulted in a significant increase in G' up to 890 ± 32 and 1205 ± 7 Pa respectively. Consistent with microscopy images (figure 2), showing an increase in material interaction or swelling, the increase in functional properties of AR suspensions upon high pressure homogenization up to 20 MPa can be attributed to an improved hydration of the cell wall fibers and rearrangement of the cell wall fiber network. The increase in pressure up to 70 MPa did not result in a further increase in G'-values, whereas no changes in microstructure occurred. It is suggested that increases in homogenization pressure above 20 MPa did not affect functionality any further. As a consequence, high pressure homogenization at 20 MPa was found to be sufficient to improve the functional properties of the AR suspensions. Therefore high pressure homogenization at 20 MPa was selected as maximal homogenization pressure for further experimental work.

3.2 Effect of pH and sequence of unit operations

To investigate the effect of pH on the viscoelastic and microstructural characteristics of AR suspensions, pH adjustments were performed ranging from pH 2.5 to pH 10. As a consequence of this pH adjustment, the sample suspensions were characterized by different sodium carbonate content, and thus potentially different electrical conductivity. Therefore, the electrical conductivity of AR suspensions adjusted to different pH values and processed according to the experimental sequences 1, 2, and 3 (figure 1) was measured (table 2). When considering the same pH value, similar conductivity values were obtained regardless of the sequence of processing operations (figure 1, sequence 1, 2, and 3). Interestingly, due to the increasing amount of Na_2CO_3 added to the AR suspensions, the increase in pH from 2.5 to 10 did not result in a progressive increase in conductivity. In particular, AR

suspensions adjusted to pH values ranging from 2.5 to 7 were characterized by similar conductivity values of about 2-4 mS/cm. By contrast, the AR suspensions adjusted to pH 10 were characterized by higher conductivity values of about 8-10 mS/cm. Since the electrical conductivity is dependent on the concentration as well as the mobility of the ions in solution, the results suggest that lemon peel acid insoluble fibers act as a buffer and can bind the ions present in solution thus limiting their mobility. In particular, up to pH 7 the binding capacity of the fibers (i.e. most likely the residual pectin fraction) resulted in negligible changes in conductivity despite the increase in ion concentration due to the higher amount of Na_2CO_3 added to the suspensions. On the other hand, at pH 10 the addition of extra ions appears to reach a concentration beyond the binding capacity of the fibers, giving reason for the increase in conductivity.

The adsorption of ions on the surface of the fibers as well as the different pH conditions might influence the AR material interactions, for instance due to electrostatic forces. As a consequence also the microstructure as well as the functionality of the AR suspensions might be affected upon processing. Therefore, the microstructure of the AR suspensions prepared according to the different sequences of processing operations (figure 1, sequence 1, 2, 3, and 4), non-homogenized and homogenized at 20 MPa, was investigated by light microscopy in DIC mode (figure B, supplementary data). The microstructure was also investigated by epifluorescence microscopy of AR suspensions stained with acridine orange (figure 4). The lower color intensity in the micrographs of the AR suspensions adjusted to pH 10 is due to the effect of pH on the cationic dye. Despite the use of the dye, epifluorescence microscopy did not reveal additional information on the microstructure of the samples. Since similar observations were made under normal and epifluorescent light, results are discussed based on the epifluorescent microscopy images shown in figure 4.

When considering the blended non-homogenized samples (AR-pH-UT and AR-UT-pH, 0 MPa) (figure 4), the micrographs show that different pH values resulted in differences in the AR suspension microstructure. In particular, in the AR suspensions adjusted to pH 2.5 (close to the original pH of the AR) some particle clusters could be visually observed under epifluorescent microscopy. On the contrary, in the micrographs of the AR suspensions adjusted to the other pH values (4.5-10) more uniformly distributed particles were observed. It is noteworthy that no clear differences in microstructure were detected depending on the sequence of pH adjustment and blending operations, suggesting that pH influenced the effect of low mechanical shear (blending) on the lemon peel acid insoluble fibers to a limited extent. The samples that were not subjected to the blending operation (AR-pH-HPH, 0 MPa) showed larger particle clusters than the blended samples (AR-pH-UT-HPH and AR-UT-pH-HPH, 0 MPa). Upon blending, it is suggested that the particle clusters were disintegrated due to the shearing forces applied. In contrast to the blended samples, no clear differences could be discerned between the different pH conditions for the non-blended samples. Upon high pressure homogenization (20 MPa) an overall disruption of the particles and particle clusters was observed. In correspondence with the work of Alvarez-Sabatel et al. (2015) and Farzi et al. (2015), it is suggested

that particle (cluster) disintegration rather than fiber depolymerization occurs upon HPH, resulting in an increased particle specific area allowing an increased interaction. In particular, in the blended and homogenized samples (AR-pH-UT-HPH and AR-UT-pH-HPH, 20 MPa) adjusted to pH 2.5 and 10, some inhomogeneous interaction of the disrupted material is suggested. On the other hand, the samples adjusted to pH 4.5, 5.5, and 7 showed a more uniform distribution of the disrupted material. With regard to the non-blended homogenized samples (AR-pH-HPH, 20 MPa) (figure 4), the micrographs of the AR suspensions adjusted to pH 5.5 showed a uniformly distributed disrupted material, whilst the micrographs of the AR suspensions adjusted to pH 2.5, 4.5, 7, and 10 showed the presence of less homogeneous distribution of the fibers. According to the present microscopy observations, pH seemed to affect the microstructure of the homogenized AR fibers by favoring fiber interaction or swelling. This behavior is mainly observed for AR suspensions adjusted to pH 4.5, 5.5, and 7 showing a more homogeneous distribution of the fibers, which can be tentatively attributed to electrostatic interactions among the fibers. However, the effect of pH on the microstructure of the homogenized AR suspensions was found to be different whether the AR suspensions were subjected (either before or after pH adjustment) or not to blending prior to homogenization.

To confirm the effect of pH on the microstructural changes of the lemon peel acid insoluble fibers during homogenization, the microstructure of AR adjusted to pH 4.5, blended, and readjusted to pH 2.5 prior to homogenization at 20 MPa was also investigated by light and epifluorescence with acridine orange microscopy (figure 5). By comparing the non-homogenized (0 MPa) AR suspension micrographs in figure 5 with those reported in figure 4 (AR-pH 4.5-UT-HPH, 0 MPa), it is apparent that the second pH adjustment resulted in a significant inhomogeneous distribution of the lemon peel acid insoluble fibers. Upon high pressure homogenization (20 MPa) (figure 5), a decrease in the clump size was observed. However, the fiber matrix seemed not as uniform as in the micrographs of the AR suspension adjusted at pH 4.5, blended and homogenized (AR-pH 4.5-UT-HPH, 20 MPa) (figure 4), thereby indicating the importance of pH at the moment of high pressure homogenization.

The effect of pH and sequence of processing operations on the microstructure of the AR suspensions was further investigated by laser diffraction analysis in which samples were compared based on their median particle diameter (table 3). In general, the median particle diameter of the non-homogenized (0 MPa) AR suspensions was larger than that of the corresponding homogenized (20 MPa) suspensions, regardless of the pH and sequence of processing operations. In good agreement with the microscopic characterization, a disintegration of the particle material was suggested upon high pressure homogenization due to the shearing forces applied. When considering the effect of pH on the median particle diameter, no clear effect could be observed in the blended non-homogenized AR suspensions (AR-pH-UT-HPH and AR-UT-pH-HPH, 0 MPa). In particular, a slight decrease in the median particle diameter with increasing pH values was observed when the pH of the AR suspension was adjusted prior to blending (AR-pH-UT-HPH, 0 MPa) (table 3). On the other hand, a similar median particle diameter was obtained when the pH of the AR suspensions was adjusted following blending (AR-UT-

pH-HPH, 0 MPa) (table 3). By contrast, when the AR suspension adjusted to pH 4.5 and blended (0 MPa) was readjusted to pH 2.5, a larger particle diameter than that of the corresponding non-readjusted suspension was observed. This result is consistent with the inhomogeneous fiber interaction observed under light and epifluorescence microscopy (figures 4 and B, supplementary data) and supports the hypothesis of different electrostatic interactions among the AR fibers at different pH conditions. With regard to the non-blended AR suspensions, consistent with the microscopy observation (figures 4 and B, supplementary data), the median particle diameter of the non-homogenized samples (AR-pH-HPH, 0 MPa) was larger than that of the blended non-homogenized samples (AR-pH-UT-HPH and AR-UT-pH-HPH, 0 MPa). In particular, a larger particle diameter was found for the AR suspensions adjusted to pH 2.5, 4.5 and 7 (table 3). On the other hand, the homogenized AR suspensions resulted in similar particle sizes, whether the homogenization was preceded or not by blending, with the only exception of the AR suspension adjusted to pH 10. In the latter case, the AR suspensions were characterized by a slightly higher particle diameter than the suspensions adjusted to the other pH values. It is remarkable that no effect of pH, nor sequence of processing conditions could be observed on the median particle diameter of the homogenized AR suspensions. On the basis of these results, it can be hypothesized that different pH conditions can lead to differences in AR suspensions as a consequence of electrostatic interactions and hydration properties of the fibers.

The effect of pH and sequence of processing operations on the technological properties of the AR suspensions was investigated by rheological analysis. First, strain sweep experiments were performed at a constant shear strain of 1 % to determine the linear viscoelastic regions of the differently processed AR suspensions (figure C, supplementary data). Within this region, frequency sweep experiments were performed at a constant angular frequency of 6.28 rad/s (figure D, supplementary data). All the samples were characterized by the storage modulus (G') higher than the loss modulus (G"). The elastic versus viscous contribution was quantified by the ratio between G" and G' (tan δ). All samples, regardless of the pH and sequence of processing operations processing, exhibited a similar value of tan δ of 0.2, which is consistent with pronounced dominance of the elastic response (data not shown). Therefore, the functionality of the different samples was compared based on the G' value corresponding to 6.28 rad/s angular frequency as G' was found to be rather independent of frequency (figure 6). By comparing the G' values of the non-homogenized AR suspensions (AR-pH-UT-HPH, AR-UT-pH-HPH, and AR-pH 4.5-UT-pH-HPH, 0 MPa) (figure 6), a clear effect of pH as well as sequence of unit operations on the functionality of the samples could be observed. In particular, the functionality of the AR suspensions adjusted to pH 2.5 was generally the lowest. On the other hand, the AR suspensions adjusted to the other pH values, before or after blending, showed better functionality, with G' values ranging from about 100 to 350 Pa. For the non-blended AR suspensions (AR-pH-HPH, 0 MPa), a very low functionality was observed at each pH value (G'< 100 Pa) prior to homogenization. It is worth noting that the AR suspension adjusted to pH 4.5, blended,

and readjusted to pH 2.5 (AR-pH 4.5-UT-pH-HPH, 0 MPa) resulted in lower functionality than the corresponding AR suspensions adjusted to pH 2.5 and 4.5 and blended (before or after pH adjustment). These results suggest that, to some extent, the pH determined the sensitivity of the lemon peel acid insoluble fibers to low shearing forces.

Upon homogenization at 20 MPa, a general increase in functionality of the AR supensions was observed (figure 6). Such increase in G' values seemed to depend on both the pH of the suspensions and the processing operations preceding the high pressure homogenization. More specifically, homogenization of the blended AR suspensions (AR-pH-UT-HPH and AR-UT-pH-HPH, 20 MPa) (figure 6) resulted in the highest G' values for pH values ranging from 4.5 to 7. Lower G' values were obtained for the AR adjusted to pH 10 and 2.5, the latter being the lowest. By contrast, no effect of the sequence of processing operations was observed. On the other hand, the non-blended and homogenized AR suspensions (AR-pH-HPH, 20 MPa) where characterized by lower functionality and a different dependency of G' on the pH. In particular, the AR adjusted to pH 5.5 and directly homogenized showed the highest functionality, followed by the AR suspension adjusted to pH 4.5, and ultimately by the AR suspensions adjusted to pH 10, 7 and 2.5. In addition, when the AR suspension was adjusted to pH 4.5, blended and readjusted to pH 2.5 prior to homgenization, a lower G' value than that of the AR suspension homogenized at pH 4.5 (AR-pH-UT-HPH and AR-UT-pH-HPH, 20 MPa) was obtained (figure 6).

According to the presented results, the pH of the suspension played a crucial role in determining the effect of high pressure homogenization on the viscoelastic behaviour of the lemon peel acid insoluble fiber suspensions. In this regard, the increase in rheological properties can be linked to a higher water holding capacity of the lemon peel acid insoluble fibers (Kunzek et al., 2002; Van Buggenhout et al., 2015). In particular, different pH values would determine different charge state of the fibers, and more specifically of the residual pectin. Pectin polymers are neutral at pH lower than 3.5, and become anionic at higher pH values. The electrostatic interactions (repulsion) occurring among the charged polymers, at pH higher than 3.5, would assist the mechanical disintegration and unfolding of the fibers upon high pressure homogenization, thus determining an increase in the water holding capacity of the fibrous matrix and higher G' values of the AR suspensions. Nevertheless, the increase in G' as a function of pH was not progressive. Therefore, these results suggest that pH is not the only system property affecting the electrostatic interactions among the lemon peel acid insoluble fibers. In fact, due to further addition of Na_2CO_3, the adjustment of the pH concomitantly resulted in different salt (ion) concentration in the AR suspensions. The presence of an excessive amount of ions in solution can screen the electrostatic interactions among the fibers (Guo et al., 2016). In this regard the fibers are not likely to be charged at pH 2.5 and thus no electrostatic repulsion or interaction occurs among them. On the other hand at pH values ranging between 4.5 and 7, the increase in the fiber charge and ion content would couterbalance one another, thus resulting in similar values of G' (figure 6) and conductivity (table 2) of the AR suspensions. Finally, at pH 10 the excess ions present in solution would screen the

fiber charges thus resulted in lower electrostatic repulsions, lower G' values and higher conductivity of the AR suspension. To verify this hypothesis, the effect of the addition of salts, namely NaCl and $CaCl_2$, on the microstructure and rheological properties of the lemon peel acid insoluble fiber suspensions was investigated.

3.3 Effect of salts

To this aim, AR suspensions were adjusted to pH 4.5 while NaCl or $CaCl_2$ were added until a conductivity value of 8 mS/cm was obtained. Subsequently, the suspensions were blended and homogenized at 20 MPa or not (0 MPa). Additional control samples were prepared by adjusting the AR suspension to pH 10, also resulting in a conductivity of 8 mS/cm, or pH 4.5, followed by blending (0 MPa) and homogenized at 20 MPa.

The microstructure of the AR suspensions was investigated by light microscopy (data not shown) and epifluorescence with acridine orange microscopy (figure 7). Similar to what was observed previously (figures B (supplementary), 4, and 5), micrographs of the non-homogenized AR suspensions (AR-pH 4.5-UT-HPH, AR-pH 10-UT-HPH, AR-pH 4.5-cond NaCl-UT-HPH and AR-pH 4.5-cond $CaCl_2$-UT-HPH, 0 MPa) show the presence of undisrupted particle clusters (figure 7). No clear effect of the addition of NaCl could be observed in the non-homogenized AR suspension adjusted to pH 4.5. By contrast, the addition of $CaCl_2$ to the AR suspension adjusted to pH 4.5 resulted in an inhomogeneous interaction of the particle fragments. Upon high pressure homogenization, an overall disruption of the matrix was observed by microscopy analysis. Consistently with what was previously observed, the AR suspension adjusted to pH 4.5 blended and homogenized at 20 MPa resulted in homogeneously disrupted material. On the other hand, the addition of both NaCl and $CaCl_2$, as well as the adjustment to pH 10 resulted in a less homogeneous interaction of the disrupted material.

The microstructure of the AR suspensions was further characterized by laser diffraction analysis. Also in this case, the average D_{50} was considered to quantify differences among the samples (table 4). Similar to table 3, the average D_{50} of the non-homogenized AR suspensions adjusted to pH 4.5 and 10 (AR-pH4.5-UT-HPH and AR-pH10-UT-HPH, 0 MPa) was larger than that of the corresponding homogenized (20 MPa) suspensions. The decrease in particle size upon high pressure homogenization was also in this case consistent with the particle disruption observed under the microscope. With regard to the AR suspension adjusted to pH 4.5 and conductivity of 8 mS/cm with NaCl, the non-homogenized sample was characterized by slightly larger particles than the non-homogenized AR suspensions adjusted to pH 4.5 and 10. Upon homogenization, the average D_{50} of the AR suspension to which NaCl was added decreased to similar values as those observed for the homogenized AR suspensions adjusted to pH 4.5 and 10. By contrast, the addition of $CaCl_2$ to the AR suspension adjusted to pH 4.5 resulted in a lower average D_{50} of the non-homogenized suspension, and a larger average D_{50} of the homogenized AR suspension as compared to that of the suspensions adjusted to pH 4.5 and 10. According to microscopy and laser diffraction results, the addition of different salts

451 determined different fiber-fiber interaction and consequently different effects on the microstructure of
452 the lemon peel acid insoluble fibers.
453 The effect of the addition of salts on the viscoelastic properties of the non-homogenized and
454 homogenized AR suspensions was investigated by rheological analysis, being by strain and frequency
455 sweep analysis (Figure C and D, supplementary data). The G' values, obtained at a constant shear
456 strain of 1 % and angular frequency of 6.28 rad/s), of the different samples are presented in figure 8.
457 Small differences in G' values were observed for the non-homogenized suspensions, with the G' of
458 AR adjusted to pH 4.5 (AR-pH 4.5-UT-HPH, 0 MPa) being the highest, and the G' of AR adjusted to
459 pH 4.5 and conductivity of 8 mS/cm with $CaCl_2$ (AR-pH 4.5-cond $CaCl_2$-UT-HPH, 0 MPa) the lowest.
460 Upon homogenization, an overall increase in functionality of the suspensions was observed, however
461 to a different extent. In particular, the AR suspension adjusted to pH 4.5 without conductivity
462 adjustment showed the highest functionality. As previously observed, homogenization of the AR
463 suspension adjusted to pH 10 resulted in lower G' values than that for pH 4.5, as a consequence of
464 different fiber-fiber electrostatic interactions. Similarly, the addition of salts to the AR suspension
465 resulted in a decrease in the functionality of the bulk sample. These results support the hypothesis that
466 not only pH but also the ion concentration are important factors determining the functionality of lemon
467 peel acid insoluble fiber suspensions upon high pressure homogenization. In particular, addition of
468 NaCl and $CaCl_2$ determined an increase in ion concentration of the AR suspension without affecting
469 the pH. Under these system properties, the excessive amount of ions present in solution would screen
470 the charges on the polymer surface and decrease the fiber repulsion. In addition, it should be noted that
471 the addition of $CaCl_2$ had a more detrimental effect than the addition of NaCl. In this regard, divalent
472 ions (Ca^{2+}) could generate intermolecular interactions between residual pectin polymers in the AR
473 suspension, thus resulting in a more compact fiber network with lower hydration capacity (Guo et al.,
474 2016; Smidsrød & Haug, 2007).

475 **4. Conclusions**

476 From the current research, it was concluded that changes in the intrinsic system properties, namely pH
477 and the concentration of salts, greatly influence the viscoelastic properties of the lemon peel acid
478 insoluble fibers upon high pressure homogenization. Moreover, the effect of pH and salts on the
479 microstructure and viscoelasticity of lemon peel acid insoluble fiber suspensions was attributed to
480 changes in electrostatic forces governing fiber interactions. These changes in intrinsic system
481 properties affected the different processing operations, being blending and high pressure
482 homogenization, to a different extent. In particular, the intrinsic system properties affected the
483 blending step to a very limited extent, resulting in rather low viscoelastic properties (G'< 400 Pa)
484 while both pH and salts played a crucial role upon high pressure homogenization of the lemon peel
485 acid insoluble fibers. Furthermore, it is suggested that above pH 3.5 the residual pectin polymers are
486 negatively charged, governing negative charges on the lemon peel acid insoluble fibers. Between pH
487 4.5 and 7, it is hypothesized that the fibers are able to undergo electrostatic interactions with the

present salts and AR material, leading to a conductivity of 2-4 mS/cm. Between these conductivity values, it was hypothesized that negative charges between the fibers favored their separation upon high pressure homogenization, thereby increasing the viscoelastic properties of the fiber suspensions. By contrast, a high salt concentration, obtained after pH adjustment to pH 10 or after excessive addition of NaCl or $CaCl_2$, was found to shield the repulsive interactions, thereby decreasing the functionality of AR fibers. In addition, blending turned out to be a necessary pre-homogenization step to obtain the greatest functionality of the suspensions, regardless of the system properties.

Finally, the presented results suggest that the tightly packed fiber network composed of lemon peel acid insoluble fibers can be unlocked when properly adjusting system properties and processing parameters, thus improving the technological properties of the fibers. In addition, the functionality of the lemon peel acid insoluble fibers could be steered by choosing specific system properties and processing sequences in order to obtain ingredients or food products with tailor made technological functionality. However, further in depth research concerning the hydration properties of functionalized lemon peel acid insoluble fibers is suggested.

5. Acknowledgements

This research was financially supported by the Institute for the Promotion of Innovation through Science and Technology (IWT) funding, project (IWT/140439/O&O).

ACCEPTED MANUSCRIPT

6. References

Alvarez-Sabatel, S., Martinez de Maranon, I., & Arboleya, J.-C. (2015). Impact of high pressure homogenisation (HPH) on inulin gelling properties, stability and development during storage. *Food Hydrocolloids*, *44*, 333–344.

Augusto, P. E. D., Ibarz, A., & Cristianini, M. (2013). Effect of high pressure homogenization (HPH) on the rheological properties of tomato juice: Creep and recovery behaviours. *Food Research International*, *54*, 169–176.

Cosgrove, D. J. (2005). Growth of the plant cell wall. *Nature Reviews. Molecular Cell Biology*, *6*, 850–861.

Cosgrove, D. J. (2014). Re-constructing our models of cellulose and primary cell wall assembly. *Current Opinion in Plant Biology*, *22*, 122–131.

Dumay, E., Chevalier-Lucia, D., Picart-Palmade, L., Benzaria, A., Gràcia-Julià, A., & Blayo, C. (2013). Technological aspects and potential applications of (ultra) high-pressure homogenisation. *Trends in Food Science & Technology*, *31*, 13–26.

Farzi, M., Yarmand, M. S., Safari, M., Emam-Djomeh, Z., & Mohammadifar, M. A. (2015). Gum tragacanth dispersions: Particle size and rheological properties affected by high-shear homogenization. *International Journal of Biological Macromolecules*, *79*, 433–439.

Floury, J., Legrand, J., & Desrumaux, A. (2004). Analysis of a new type of high pressure homogeniser. Part B. study of droplet break-up and recoalescence phenomena. *Chemical Engineering Science*, *59*, 1285–1294.

Foster, T. J. (2011). Natural structuring with cell wall materials. *Food Hydrocolloids*, *25*, 1828–1832.

Guo, X., Meng, H., Tang, Q., Pan, R., Zhu, S., & Yu, S. (2016). Effects of the precipitation pH on the ethanolic precipitation of sugar beet pectins. *Food Hydrocolloids*, *52*, 431–437.

Kunzek, H., Müller, S., Vetter, S., & Godeck, R. (2002). The significance of physico chemical properties of plant cell wall materials for the development of innovative food products. *European Food Research and Technology*, *214*, 361–376.

Lamport, D. T. a, Kieliszewski, M. J., Chen, Y., & Cannon, M. C. (2011). Role of the extensin superfamily in primary cell wall architecture. *Plant Physiology*, *156*, 11–19.

Lopez-Sanchez, P., Nijsse, J., Blonk, H. C. G., Bialek, L., Schumm, S., & Langton, M. (2011). Effect of mechanical and thermal treatments on the microstructure and rheological properties of carrot, broccoli and tomato dispersions. *Journal of the Science of Food and Agriculture*, *91*, 207–17.

Paquin, P. (1999). Technological properties of high pressure homogenizers: the effect of fat globules, milk proteins, and polysaccharides. *International Dairy Journal*, *9*, 329–335.

Sampedro, J., & Cosgrove, D. J. (2005). The expansin superfamily. *Genome Biology*, *6*, 242.

Sankaran, A. K., Nijsse, J., Bialek, L., Bouwens, L., Hendrickx, M. E., & Van Loey, A. M. (2015). Effect of Enzyme Homogenization on the Physical Properties of Carrot Cell Wall Suspensions. *Food and Bioprocess Technology*, *8*, 1377–1385.

Sankaran, A. K., Nijsse, J., Bialek, L., Shpigelman, A., Hendrickx, M. E., & Van Loey, A. M. (2015). Enhanced electrostatic interactions in tomato cell suspensions. *Food Hydrocolloids*, *43*, 442–450.

Shpigelman, A., Kyomugasho, C., Christiaens, S., Van Loey, A. M., & Hendrickx, M. E. (2014). Thermal and high pressure high temperature processes result in distinctly different pectin non-enzymatic conversions. *Food Hydrocolloids*, *39*, 251–263.

Smidsrød, O., & Haug, A. (2007). Precipitation of acidic polysaccharides by salts in ethanol-water mixtures. *Journal of Polymer Science Part C: Polymer Symposia*, *16*, 1587–1598.

Tan, J., & Kerr, W. L. (2015). Rheological properties and microstructure of tomato puree subject to continuous high pressure homogenization. *Journal of Food Engineering*, *166*, 45–54.

Van Buggenhout, S., Wallecan, J., Christiaens, S., Debon, S. J. J., Desmet, C., Van Loey, A., … Mazoyer, J. (2015). Influence of high-pressure homogenization on functional properties of orange pulp. *Innovative Food Science & Emerging Technologies*, *30*, 51–60.

Verrijssen, T. A. J., Vanierschot, M., Ongena, S. I. M., Cardinaels, R., Van den Bulck, E., Van Loey, A. M., … Van Buggenhout, S. (2014). Role of mechanical forces in the stomach phase on the in vitro bioaccessibility of β-carotene. *Food Research International*, *55*, 271–280.

Willemsen, K. L. D. D., Panozzo, A., Moelants, K., Debon, S. J. J., Desmet, C., Cardinaels, R., … Hendrickx, M. E. G. (2017). Physico-chemical and viscoelastic properties of high pressure homogenized lemon peel fi ber fraction suspensions obtained after sequential pectin extraction. *Food Hydrocolloids*, *72*, 358–371.

Winuprasith, T., & Suphantharika, M. (2013). Microfibrillated cellulose from mangosteen (Garcinia mangostana L.) rind: Preparation, characterization, and evaluation as an emulsion stabilizer. *Food Hydrocolloids*, *32*, 383–394.

ACCEPTED MANUSCRIPT

566 **Table 1:** Median particle diameter (D_{50}) of lemon peel acid insoluble residue (AR) suspensions adjusted to pH
567 5.5, blended (UT), non-homogenized (0 MPa) and homogenized at different homogenization pressures (10 MPa
568 to 70 MPa) ± standard deviation. Significant differences (Tuckey test, $P < 0.05$) are indicated with different
569 letters.

Homogenization pressure level (MPa)	D_{50} (µm)
0	118 ± 1^{a}
10	75 ± 0^{b}
20	73 ± 0^{b}
30	78 ± 4^{b}
40	69 ± 0^{b}
50	72 ± 6^{b}
60	71 ± 8^{b}
70	75 ± 14^{b}

570

ACCEPTED MANUSCRIPT

571 **Table 2:** Electrical conductivity (mS/cm) of lemon peel acid insoluble residue (AR) suspensions adjusted to pH
572 2.5, 4.5, 5.5, 7, and 10, non-blended and blended (UT) (before or after pH adjustment), non-homogenized (0
573 MPa) and homogenized at 20 MPa.

	Conductivity (mS/cm)					
	AR-pH-UT-HPH		AR-UT-pH-HPH		AR-pH-HPH	
	0 MPa	20 MPa	0 MPa	20 MPa	0 MPa	20 MPa
pH 2.5	3.3	3.4	3.3	3.4	3.7	3.7
pH 4.5	2.5	2.3	2.6	2.3	2.7	2.6
pH 5.5	2.6	2.2	2.8	2.5	3.4	3
pH 7	3.4	3.2	3.3	2.9	3.1	3.1
pH 10	8.8	8	10.6	10	9.3	8.9

574

ACCEPTED MANUSCRIPT

575 **Table 3:** Median particle diameter (D_{50}) of lemon peel acid insoluble residue (AR) suspensions adjusted to pH
576 2.5, 4.5, 5.5, 7, and 10, non-blended and blended (UT) (before or after pH adjustment), non-readjusted or
577 readjusted to pH 2.5, non-homogenized (0 MPa) and homogenized at 20 MPa ± standard deviation. Significant
578 differences (Tukey test, $P < 0.05$) are indicated with different letters.

	D_{50} (µm)							
	AR-pH-UT-HPH		AR-UT-pH-HPH		AR-pH-HPH		AR-pH4.5-UT-pH-HPH	
	0 MPa	20 MPa	0 MPa	20 MPa	0 MPa	20 MPa	0 MPa	20 MPa
pH 2.5	133 ± 0^{def}	75 ± 0^{k}	133 ± 0^{def}	75 ± 0^{k}	188 ± 1^{b}	77 ± 1^{k}		
pH 4.5	126 ± 5^{fg}	64 ± 1^{l}	135 ± 2^{def}	70 ± 1^{kl}	212 ± 6^{a}	74 ± 0^{kl}		
pH 5.5	114 ± 1hi	68 ± 0^{kl}	127 ± 1^{de}	71 ± 0^{kl}	160 ± 2^{c}	73 ± 0^{kl}	213 ± 8^{a}	75 ± 1^{k}
pH 7	110 ± 2^{hi}	71 ± 0^{kl}	135 ± 0^{gh}	69 ± 0^{kl}	206 ± 1^{a}	70 ± 0^{kl}		
pH 10	91 ± 0^{j}	92 ± 1^{j}	119 ± 1^{gh}	92 ± 1^{j}	137 ± 0^{d}	108 ± 3^{i}		

579

ACCEPTED MANUSCRIPT

580 **Table 4:** Median particle diameter (D_{50}) of lemon peel acid insoluble residue (AR) suspensions adjusted to pH
581 4.5 and 10, conductivity of 8 mS/cm (with either NaCl or $CaCl_2$), blended (0 MPa), and homogenized at 20 MPa
582 ± standard deviation. AR suspensions at pH 4.5 and 10 without conductivity adjustment are considered as
583 controls. Significant differences (Tukey test, $P < 0.05$) are indicated with different letters.

584

	D_{50} (µm)			
	AR-pH-UT-HPH		AR-pH 4.5-cond-UT-HPH	
	pH 4.5	pH 10	NaCl	$CaCl_2$
0 MPa	110 ± 1^{a}	90 ± 1^{c}	121 ± 0^{a}	73 ± 0^{d}
20 MPa	71 ± 0^{e}	67 ± 2^{bc}	73 ± 0^{d}	99 ± 0^{b}

585

ACCEPTED MANUSCRIPT

Figure 1: Experimental set-up to study the effect of pH and addition of salts on the blending and activation of the raw material.

Figure 2: Light and epifluorescence microscopy images of lemon peel acid insoluble residue (AR) suspensions adjusted to pH 5.5, blended (UT), non-homogenized (0 MPa) and a selection of representative images of homogenized AR suspension at different homogenization pressures (10 MPa to 70 MPa). Scale bars correspond to 500 µm.

Figure 3: Storage modulus at 6.28 rad/s of lemon peel acid insoluble residue (AR) suspensions adjusted to pH 5.5, blended (UT), non-homogenized (0 MPa) and homogenized at different homogenization pressures (10 MPa to 70 MPa). Error bars represent the standard deviation. Significant differences (Tuckey test, $P < 0.05$) are indicated with different letters.

Figure 4: Epifluorescence with acridine orange microscopy images of lemon peel acid insoluble residue (AR) suspensions adjusted to pH 2.5, 4.5, 5.5, 7.0, and 10, non-blended and blended (UT) (before or after pH adjustment), non-homogenized (0 MPa) and homogenized at 20 MPa. Scale bars correspond to 500 µm.

Figure 5: Light and epifluorescence with acridine orange microscopy images of lemon peel acid residue (AR) suspensions adjusted to pH 4.5, blended (0 MPa), readjusted to pH 2.5, and homogenized at 20 MPa. Scale bars correspond to 500 µm.

Figure 6: Storage modulus at 6.28 rad/s of lemon peel acid insoluble residue (AR) suspensions adjusted to pH 2.5, 4.5, 5.5, 7, and 10, non-blended and blended (UT) (before or after pH adjustment), non-readjusted or readjusted to pH 2.5, non-homogenized (0 MPa) and homogenized at 20 MPa. Error bars represent the standard deviation. Significant differences (Tukey test, $P < 0.05$) are indicated with different letters.

Figure 3: Epifluorescence with acridine orange microscopy images of control lemon peel acid insoluble residue (AR) suspensions adjusted to pH 4.5 and 10, blended, non-homogenized (0 MPa) and homogenized at 20 MPa and AR suspensions adjusted to pH 4.5, conductivity 8 mS/cm (with either NaCl or $CaCl_2$), blended (UT), non-homogenized (0 MPa), and homogenized at 20 MPa. Scale bars correspond to 500 µm.

Figure 8: Storage modulus at 6.28 rad/s of lemon peel acid insoluble residue (AR) suspensions adjusted to pH 4.5 and 10, and conductivity of 8 mS/cm (with either NaCl or $CaCl_2$), blended (0 MPa), and homogenized at 20 MPa. No conductivity changes were made for AR suspensions at pH 4.5 and 10. Error bars represent the standard deviation. Significant differences (Tukey test, $P < 0.05$) are indicated with different letters.

ACCEPTED MANUSCRIPT

ACCEPTED MANUSCRIPT

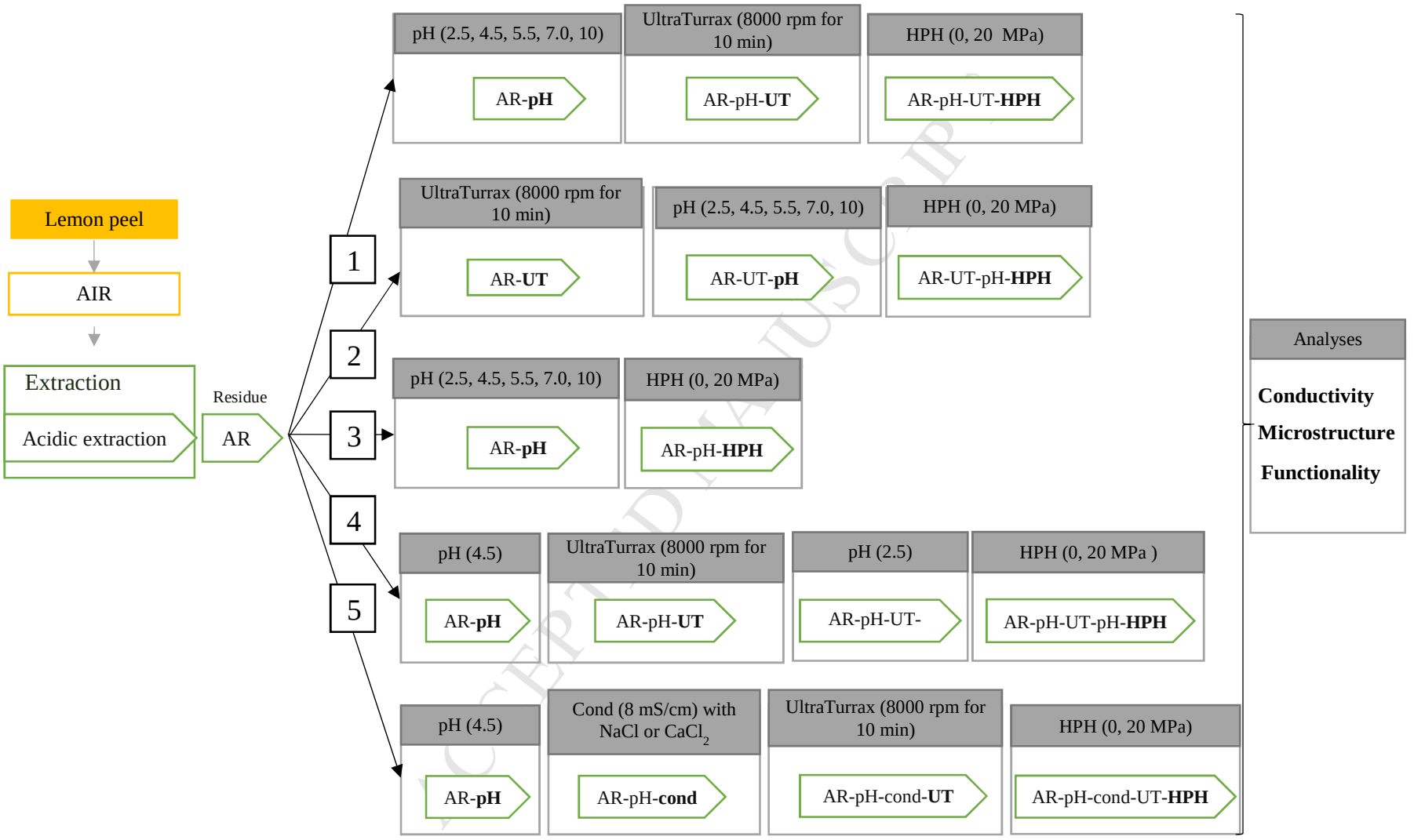

Figure 1

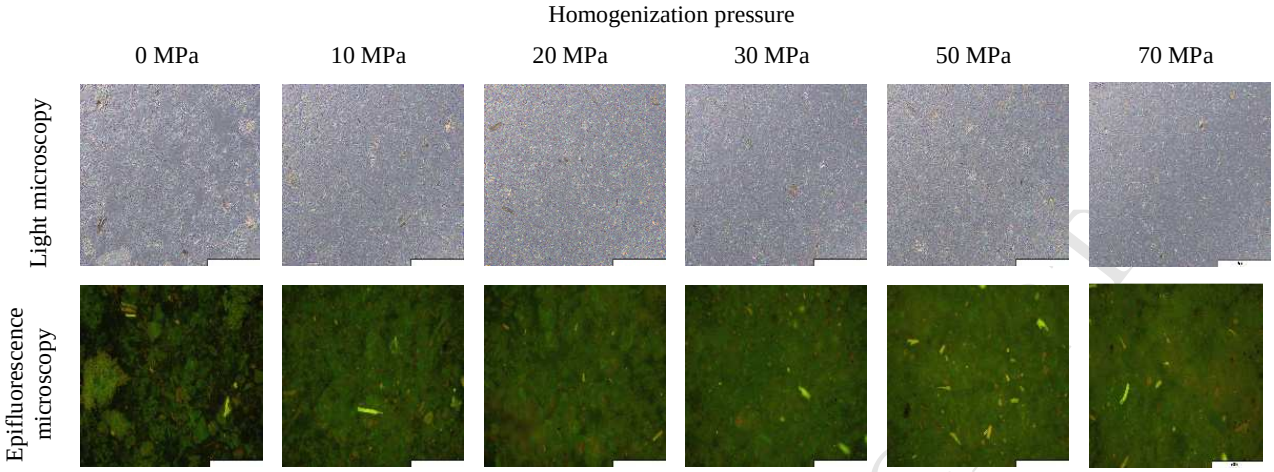

Figure 2

ACCEPTED MANUSCRIPT

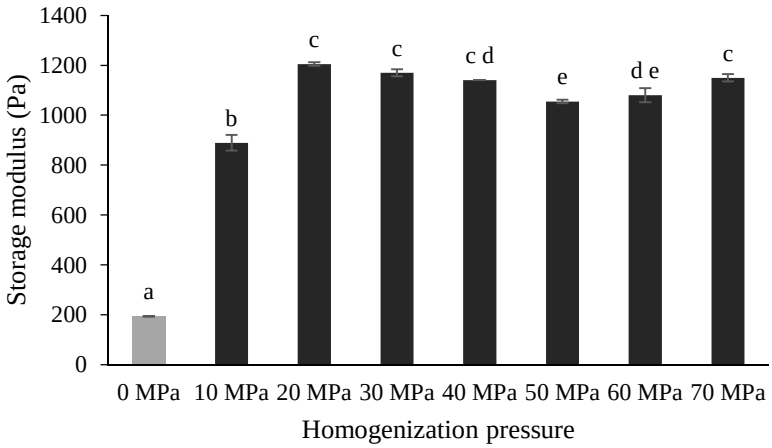

Figure 3

ACCEPTED MANUSCRIPT

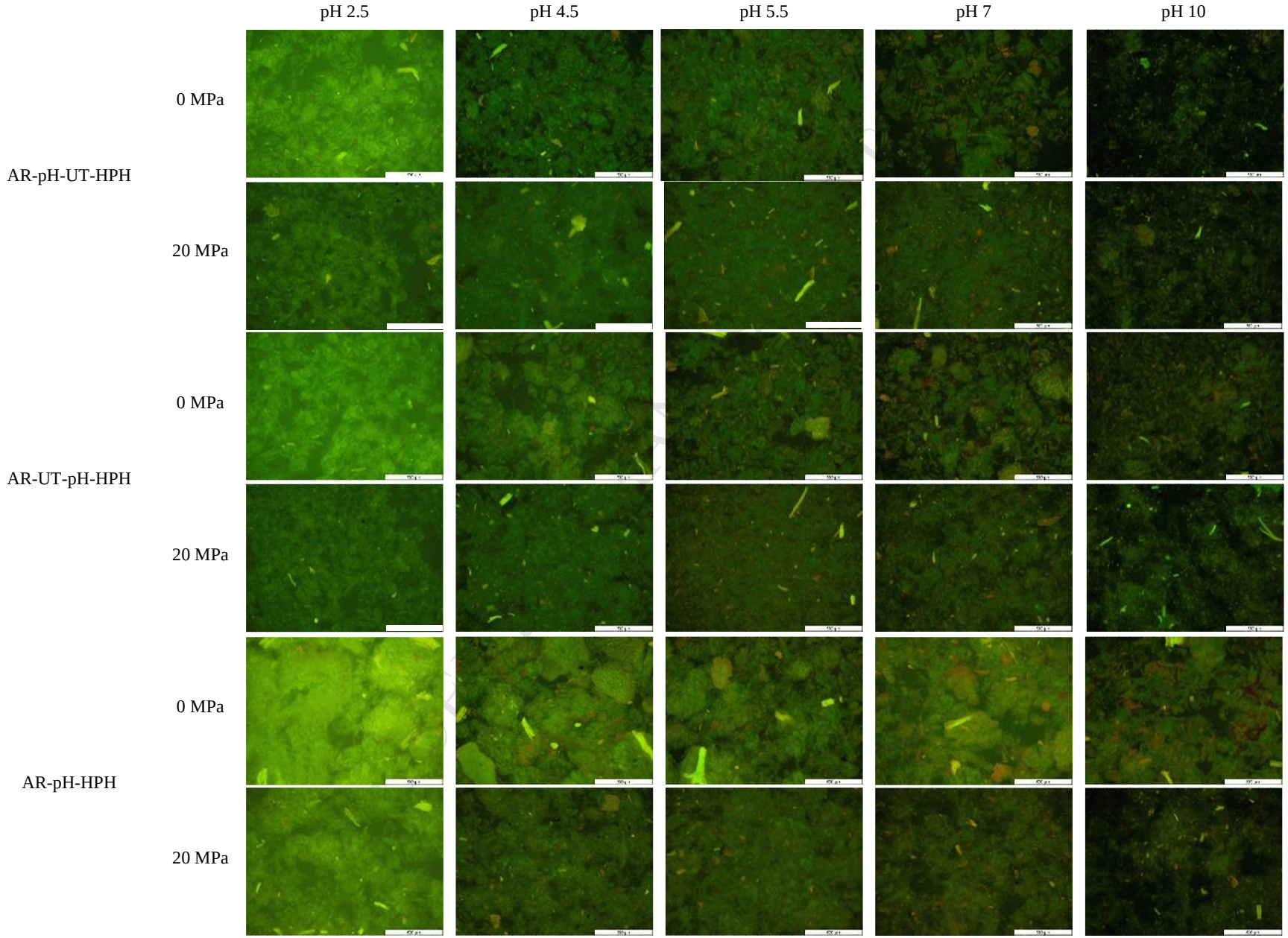
pH 2.5
pH 4.5
pH 5.5
pH 7
pH 10
AR-pH-UT-HPH
0 MPa
20 MPa
AR-UT-pH-HPH
0 MPa
20 MPa
AR-pH-HPH
0 MPa
20 MPa

Figure 4

ACCEPTED MANUSCRIPT

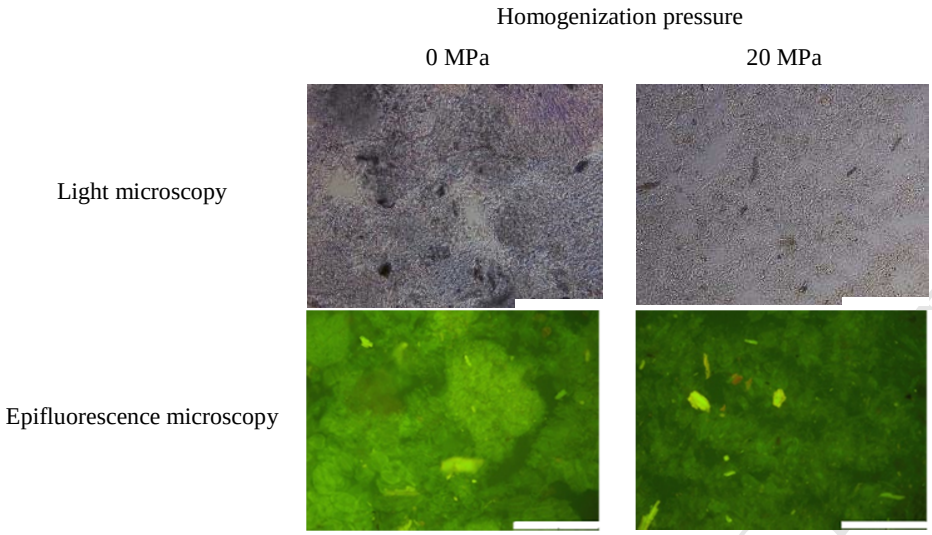

Figure 5

ACCEPTED MANUSCRIPT

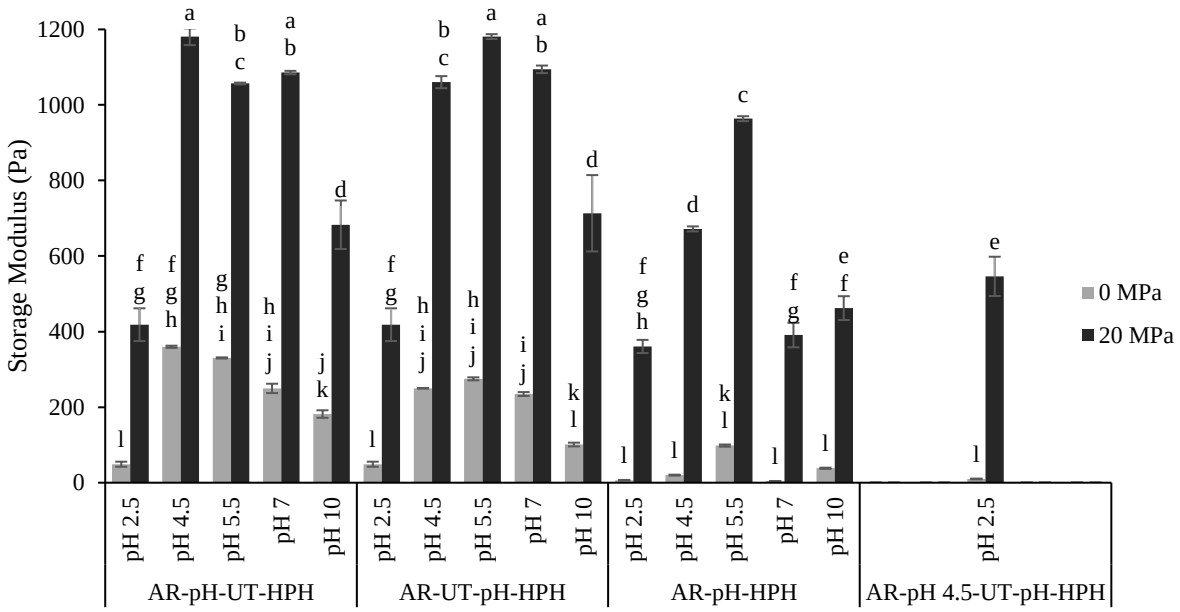

Figure 6

ACCEPTED MANUSCRIPT

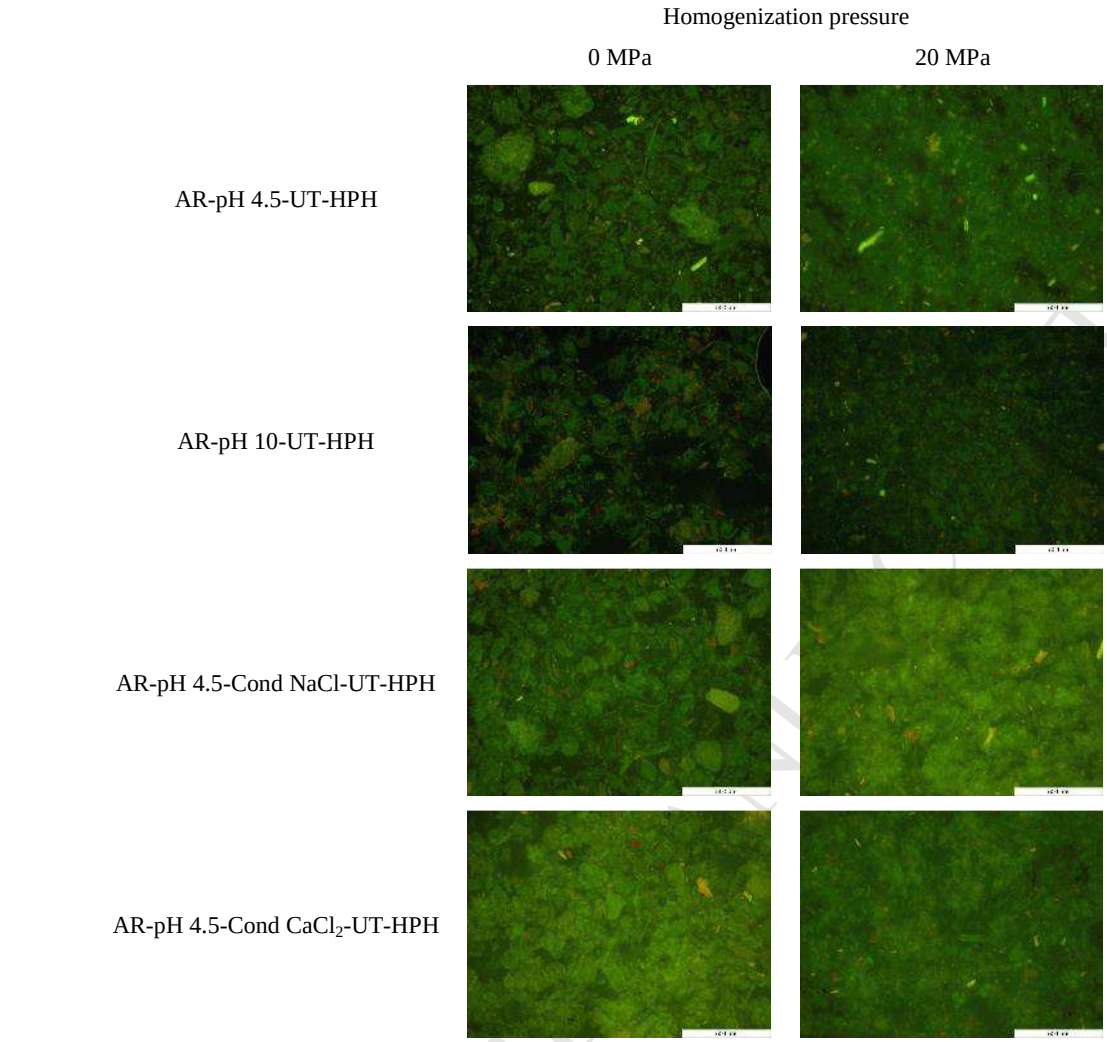

Figure 7

ACCEPTED MANUSCRIPT

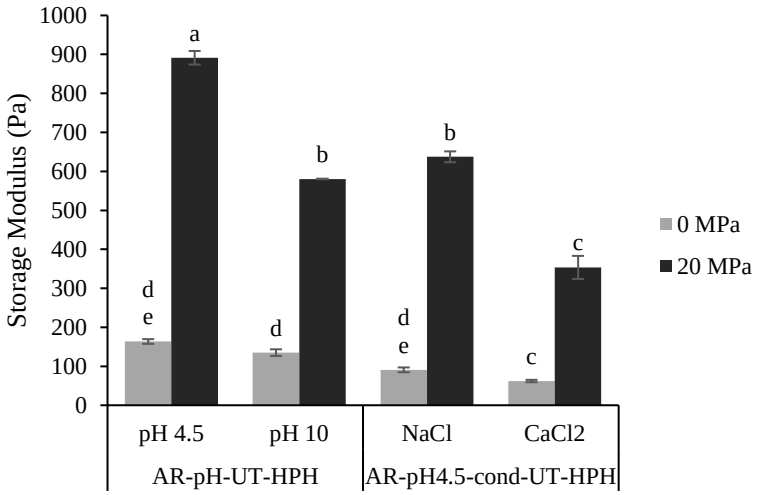

Figure 8

ACCEPTED MANUSCRIPT

ACCEPTED MANUSCRIPT

Highlights

- HPH at 20 MPa is sufficient to thicken lemon peel AR suspensions
- Blending prior to HPH results in optimal texturizing properties of AR suspensions
- pH and addition of salts are crucial to optimize the effects of HPH
- Electrostatic interactions favor the separation of AR fibers upon HPH
- Extensive salt addition negatively influences the texture of AR suspensions

ACCEPTED MANUSCRIPT